NASA TECHNICAL MEMORANDUM

NASA TM X-1316

NASA TM X-1316

N67 12808

TMX-1316

PEGASUS SATELLITE MEASUREMENTS OF METEOROID PENETRATION (FEB. 16 - DEC. 31, 1965)

by Stuart Clifton and Robert Naumann

George C. Marshall Space Flight Center

Huntsville, Ala.

NATIONAL AERONAUTICS AND SPACE ADMINISTRATION • WASHINGTON, D. C. • DECEMBER 1966

NASA TM X-1316

PEGASUS SATELLITE MEASUREMENTS OF METEOROID PENETRATION

(FEB. 16 - DEC. 31, 1965)

By Stuart Clifton and Robert Naumann

George C. Marshall Space Flight Center
Huntsville, Ala.

NATIONAL AERONAUTICS AND SPACE ADMINISTRATION

For sale by the Clearinghouse for Federal Scientific and Technical Information
Springfield, Virginia 22151 – Price $2.00

TABLE OF CONTENTS

LIST OF ILLUSTRATIONS

PEGASUS SATELLITE MEASUREMENTS OF METEOROID PENETRATION (FEB. 16 - DEC. 31, 1965)

SUMMARY

A statistically defensible criterion for the validation of Pegasus satellite data is presented in this report and the observed fluxes are calculated on this basis. The calculated values are then corrected for possible lost counts using the detectability factors determined in laboratory tests. The resulting fluxes are .00487/ m^2 day for the 0.4-mm detectors, .0209/ m^2 day for the 0.2-mm detectors, and .188/ m^2 day for the 0.038-mm detectors.

Analysis of the data shows neither a significant correlation of the penetration flux with hour or season nor a definite correlation with meteoric activity, although the possibility exists.

The Pegasus data points are shown in relation to other flux models, but a comprehensive discussion of this matter is deferred to a separate report.

INTRODUCTION

Three satellites, Pegasus I, II, and III, were launched on February 16, May 25, and July 30, 1965, respectively, to investigate the near-earth meteoroid environment at altitudes ranging initially from 500 to 700 kilometers above the surface of the earth. The initial orbital elements of the three spacecraft are presented in Table 1.

Each satellite has two extendable wings containing 62 groups of detector panels exposed to the meteoroid environment. Each panel group contains from two to eight individual detectors of a given aluminum target sheet thickness of either 0.038 mm, 0.2 mm, or 0.4 mm. The target sheet is the exposed surface of the detector and forms a parallel plate capacitor with a layer of vapor-deposited copper beneath a 12-micron mylar dielectric. The capacitors are maintained at constant voltage until shorted by impinging meteoroids. Detection of discharge and subsequent recharge, accomplished by an appropriate electronic network, signifies a penetration. The details of the Pegasus structure and operation are covered in an earlier document[1].

TABLE 1

INITIAL ORBITAL ELEMENTS OF PEGASUS SPACECRAFT

	Pegasus I	Pegasus II	Pegasus III
Period (min)	97.0	97.2	95.2
Eccentricity	0.0169	0.0164	0.0013
Inclination (deg)	31.76	31.77	28.89
Semi-major Axis (km)	6998.0	7005.3	6909.4
Perigee Height (km)	501.6	511.7	521.9
Apogee Height (km)	737.7	742.1	540.0

A number of changes from Pegasus I (reported earlier [1]) were implemented in Pegasus II. The only significant difference in the structures of Pegasus II and Pegasus III is the installation on some of the detector panels of removable coupons which may later be recovered from orbit. Because of this experiment, Pegasus III exposes slightly less area to meteoroid penetration. An area of 1.600 m^2 on the +Y wing and 4.596 m^2 on the -Y wing was inactivated for the experiment (see Appendix). All of the area lost was confined to 0.4-mm panels.

Differences in the orientation of Pegasus I and Pegasus II are covered in Reference 1. The detector plane of Pegasus I is normal to the satellite's rotational axis which precesses slowly in space under the influence of gravity gradient torques. This motion will allow some analysis of the directional distribution of meteoroid radiants when sufficient data are available.

The rotational dynamics of Pegasus II and III is such that an analysis of the directional distribution is not yet possible.

The primary mission of the spacecraft is to determine the meteoroid penetration frequency in three different thicknesses of aluminum. As of December 31, 1965, Pegasus II and III recorded 387 penetrations on the 0.038-mm detectors, 41 penetrations on the 0.2-mm detectors, and 201 penetrations on the 0.4-mm detectors. Due to anomalous behavior, the puncture rates observed by Pegasus I will be presented later in the report.

Because of panel shorting and intermittencies, the active area of each satellite has been reduced. As of December 31, 1965, a total of 18.6 m^2 of active 0.038-mm panel area remains exposed to meteoroid penetration on the three satellites. A total of 6.4 m^2 of the 0.2-mm panels and 221.5 m^2 of the 0.4-mm panels is presently considered active area for the three spacecraft.

An analysis of the meteoroid data obtained from Pegasus satellites over a period beginning with respective launches and ending December 31, 1965, is presented in this report. The flux rates are determined and a panel distribution of hits presented in Appendix A. The data will be investigated further for possible diurnal and seasonal effects and a correlation with major, known meteor showers. Also, a comparison of the results with various models is discussed.

VALIDATION OF PENETRATION DATA

Because of various unpredicted characteristics inherent in the thicker detector panels, such as intermittent and excessive permanent shorting, earlier analysis [1] involved some subjective judgment for the selection of valid events. From this experience, a more formal procedure has evolved which provides a systematic, statistically defensible method for excluding false events. Penetration frequencies are first determined using only initial penetrations of individual detectors, neglecting the area contributions of each detector after the first penetration. This eliminates the possibility of error from counting false events arising from damage associated with a previous event. A criterion which calls for the rejection of any event that occurs within one orbit of a previous event on the same panel was adopted for validating subsequent events on penetrated panels. If damage exists near a perforation that will cause intermittent shorting due to thermal cycling, it will generally occur at least once in each thermal cycle. This criterion eliminates the majority of intermittent events. However, cases have been observed in which a detector panel records fewer than one intermittent event per orbit. For this reason any detector whose flux deviates by $\pm$ 3 σ from the average frequency obtained from the remaining panels of similar thickness during any interval containing more than one event, is considered unreliable and is not used. Frequencies are then determined on the basis of total events acceptable under these criteria. If frequencies determined by both methods are in reasonable agreement, this is an indication that no substantial error has been introduced by considering the total events, and the increased number of events lowers the statistical uncertainty.

Some doubt has remained concerning the validity of those events which precipitate panel shorting or intermittency. A discussion of shorted and intermittent panels has been presented by Naumann [1] and will be omitted in the present analysis. An attempt to either confirm or reject these events as valid penetrations is made with regard to panel temperature distributions.

Up to the present time, shorting and the intermittent updating of panels has occurred primarily on the 0.2-mm and 0.4-mm panels. The shorting rate of the Pegasus 0.2-mm and 0.4-mm detectors exceeds the expected shorting rate observed by laboratory tests by over a factor of three. However, no shorting and little intermittency has been observed on the 0.038-mm detectors.

Assuming the data are random, it might be expected that the temperatures coincident with valid penetrations of the 0.038-mm panels would reflect to a high degree the distribution of temperatures recorded by the satellite panel temperature probes. The panel temperature probes, one of which is located on either side of the wing, record the panel temperatures at five minute intervals. If the rate of satellite spin is rapid enough, the temperature data recorded at five minute intervals produces an accurate representation of the observed temperature patterns. Furthermore, with a rapid spin rate, both probes record similar results such that the temperatures from both wing sides may be combined into a single distribution. The data used in this analysis is exclusively confined within periods for which each satellite experiences a rapid spin rate. For Pegasus II and III this occurs during the first three months of flight.

The temperature distributions observed by the temperature probes of Pegasus II and Pegasus III during the first three months of their respective flights are summarized in Figures 1a and 2a. Figures 1b and 2b present the panel temperatures coincident with valid penetrations of the 0.038-mm panels of the two satellites. It was found that the distribution of these latter temperatures is within acceptable statistical limits set by the expected distribution.

Assuming once again randomness of the penetration data, it is expected that the distribution of temperatures coincident with the 0.4-mm panel penetrations should also reflect within statistical limits the distribution of temperatures recorded by the probes. However, as can be seen from Figures 1c and 2c, this is the case only when those penetrations which precipitate panel shorting and intermittency are included. These penetrations occur primarily at higher temperatures, and their elimination would indicate a great lack of valid penetrations at these temperatures. Although this lack is possibly real, it is not thought likely. Therefore, for the purposes of this analysis, these penetrations which apparently cause the shorting and intermittent updating of panels will be considered valid.

OBSERVED PENETRATION FREQUENCIES

The agreement between the 0.4-mm data from Pegasus II and III initial events and total valid events is exceptionally good as may be seen in Figure 3. Therefore the data from the two satellites may be combined. The four events observed by Pegasus I make practically no contribution and are not included in the total. However, they are consistent within reasonable statistical bounds with Pegasus II and III. The two satellites have recorded 201 events for a flux of $0.0040/m^2$ day. The $\pm 1\sigma$ interval includes from $0.0037/m^2$ day to $0.0043/m^2$ day.

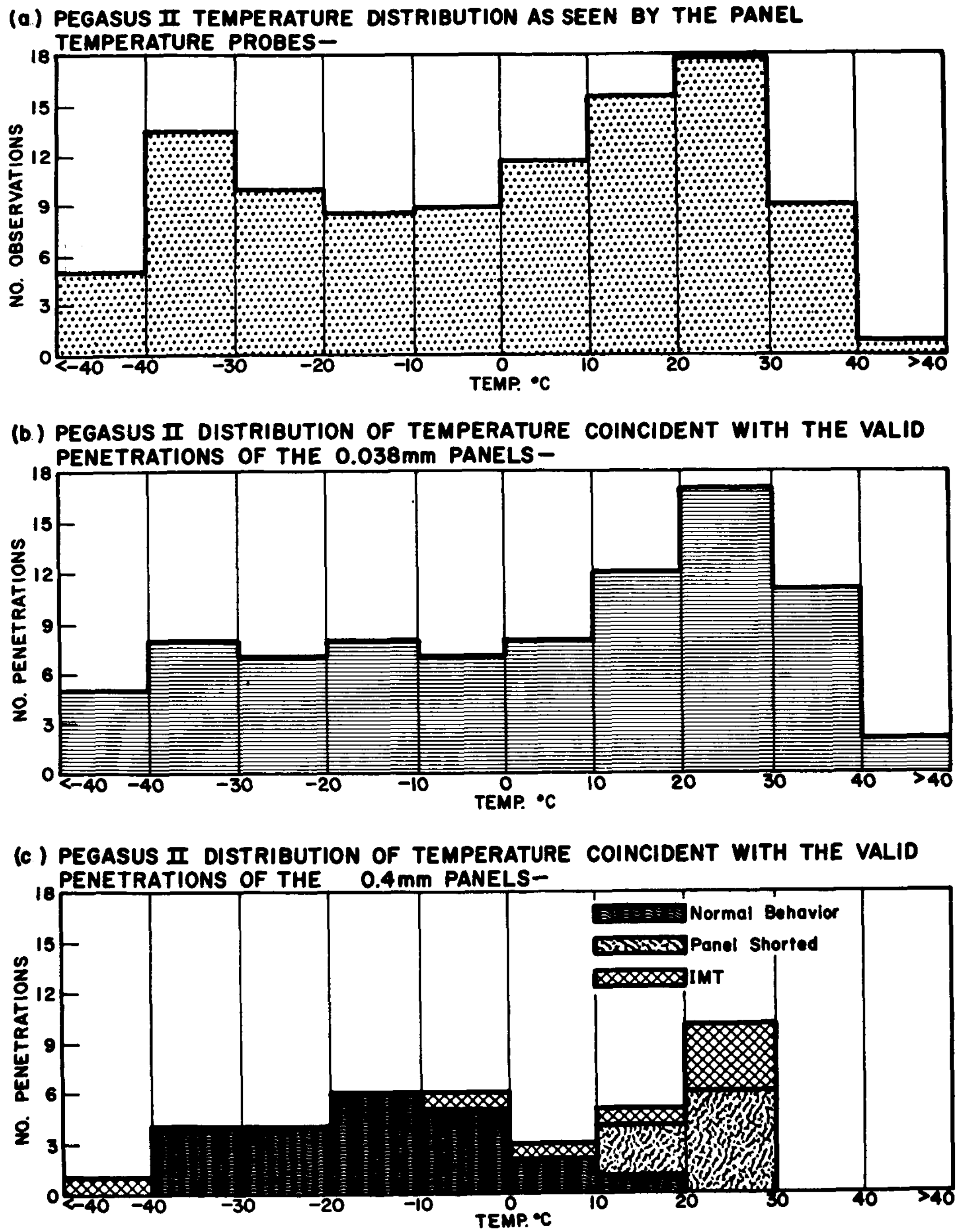

FIGURE 1. OBSERVED PEGASUS II TEMPERATURE DISTRIBUTIONS

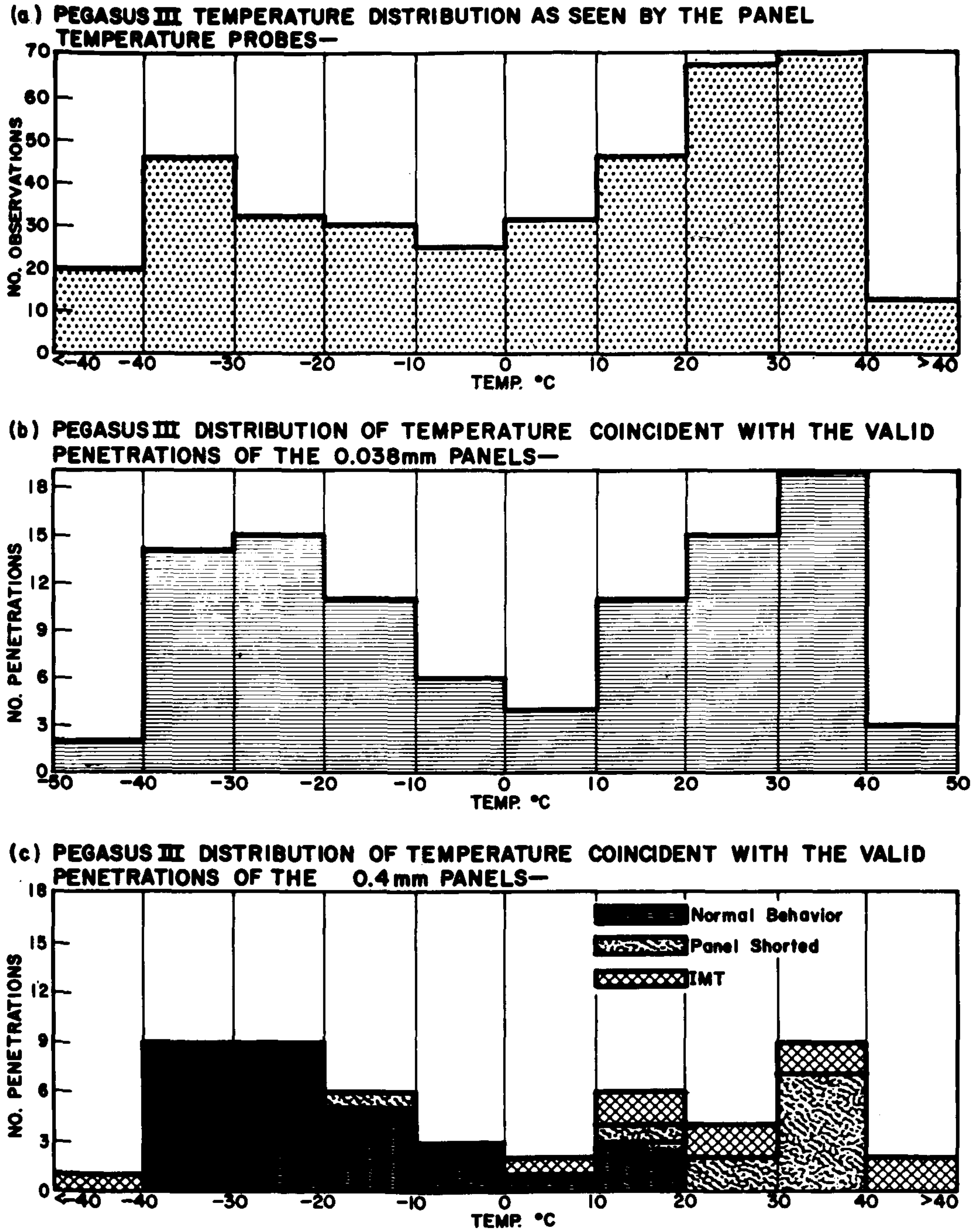

FIGURE 2. OBSERVED PEGASUS III TEMPERATURE DISTRIBUTIONS

FREQUENCIES OF PENETRATIONS - 0.4mm

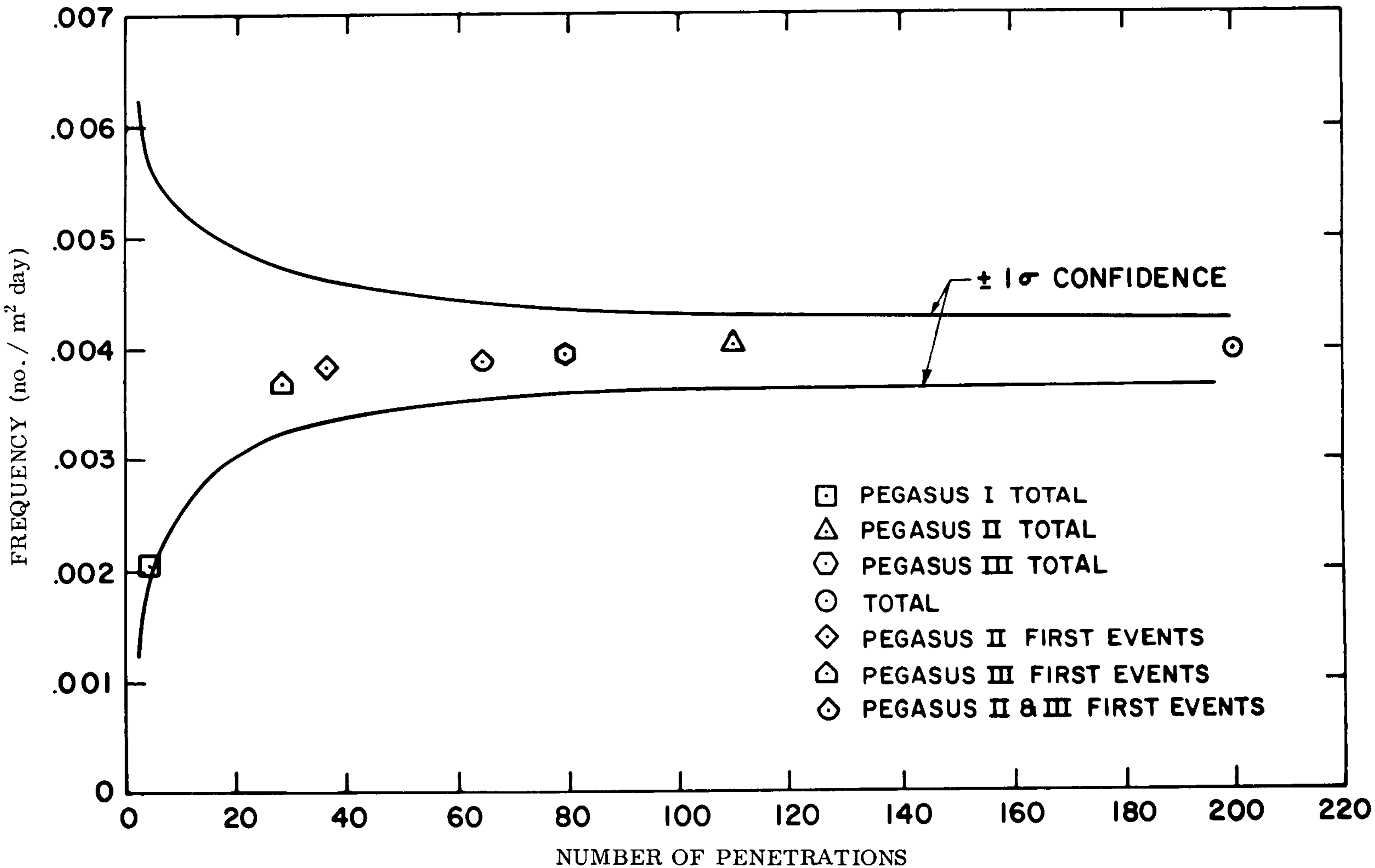

FIGURE 3. COMPARISON OF THE FREQUENCY OF 0.4-MM PANEL PENETRATIONS BETWEEN INITIAL AND TOTAL EVENTS

Figure 4 indicates that the 0.2-mm panel data from Pegasus II and III are likewise well within acceptable statistical bounds, and these data may also be combined. Since the number of 0.2-mm events for Pegasus II and III is fairly small, and since Pegasus I observed 8 events with the 0.2-mm detectors, it is desirable to include these data in the total even though Pegasus I did not provide all the diagnostic data such as panel identification and recharge time. Figure 4 shows that the penetration frequency observed by Pegasus I deviates by slightly more than 1 σ from the average of Pegasus II and III. However, it is well within 2 σ and may be considered to be within acceptable statistical bounds. The 0.2-mm panels have recorded 49 penetrations, and the average 0.2-mm penetration frequency is found to be $0.018/m^2$ day with $\pm$ 1 σ bounds of $0.021/m^2$ day and $0.015/m^2$ day.

The monthly flux of the 0.038-mm panels for each wing of each spacecraft is displayed in Table II. The data from Pegasus II and III essentially are in agreement throughout their respective flights. The data from the +Y wing on Pegasus I exhibit a five-month period for which the results are not within tolerable statistical limits. Until this behavior is better understood, these data will be omitted from consideration, although the rest of the Pegasus I 0.038-mm data are within statistical bounds and shall be included in the total. The comparison of initial and total events for the 0.038-mm detectors from the three spacecraft is shown in Figure 5. Again, it may be seen that the correlation between the initial and total events of the three satellites is in good agreement. The 0.038-mm panels have encountered 582 penetrations for a flux of $0.160/m^2$ day with $\pm$ 1 σ limits of $.167/m^2$ days and $.153/m^2$ day.

Two corrections to the quoted flux values may now be investigated. The first results from the imposition of the validation criterion presented previously. If a panel should observe two or more penetrations within an orbital period, only the first is considered valid. However, the criterion excludes the case in which the latter penetration is valid. In order to correct for the possibility of this occurrence, the area of a penetrated panel must be excluded from active area for a period of ninety-five minutes after each penetration. The correction when applied to the 0.4-mm and 0.2-mm panels does not perceptibly alter the values of penetration flux given above. However, due to the small area and large number of penetrations of the 0.038-mm panels, the corrected flux for these panels is 0.161 penetrations per m^2day.

The second correction results from the penetrations whose integrated discharge is below the limit of threshold detectability. Figures 6a and 6b present the results of the Detector Design Assurance Tests performed by Fairchild Hiller, prime contractor of the Pegasus satellites, at the Hayes International Corporation for the 0.4-mm and 0.038-mm panels.

FREQUENCY OF PENETRATIONS - 0.2mm

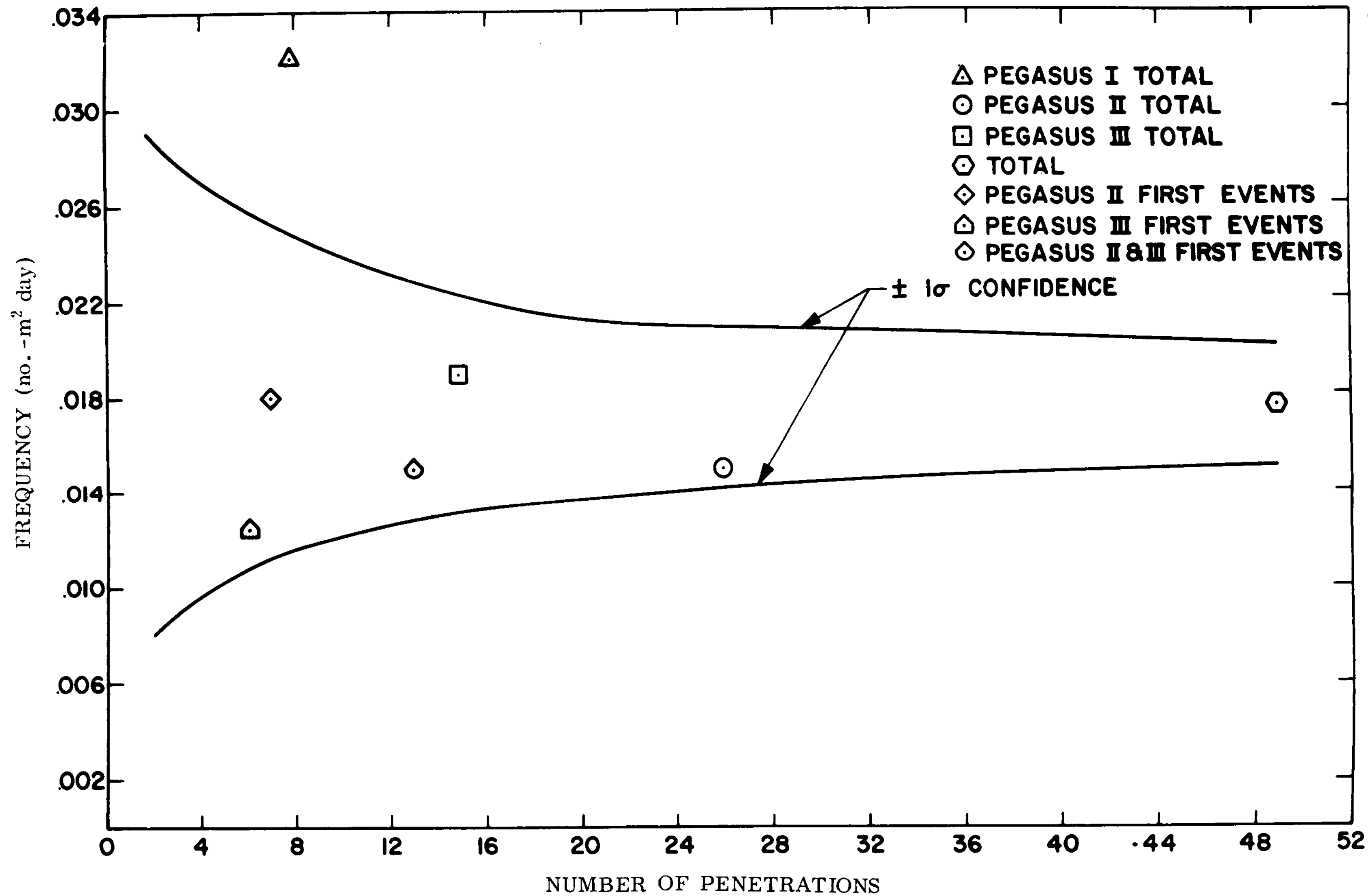

FIGURE 4. COMPARISON OF THE FREQUENCY OF 0.2-MM PANEL PENETRATIONS BETWEEN INITIAL AND TOTAL EVENTS

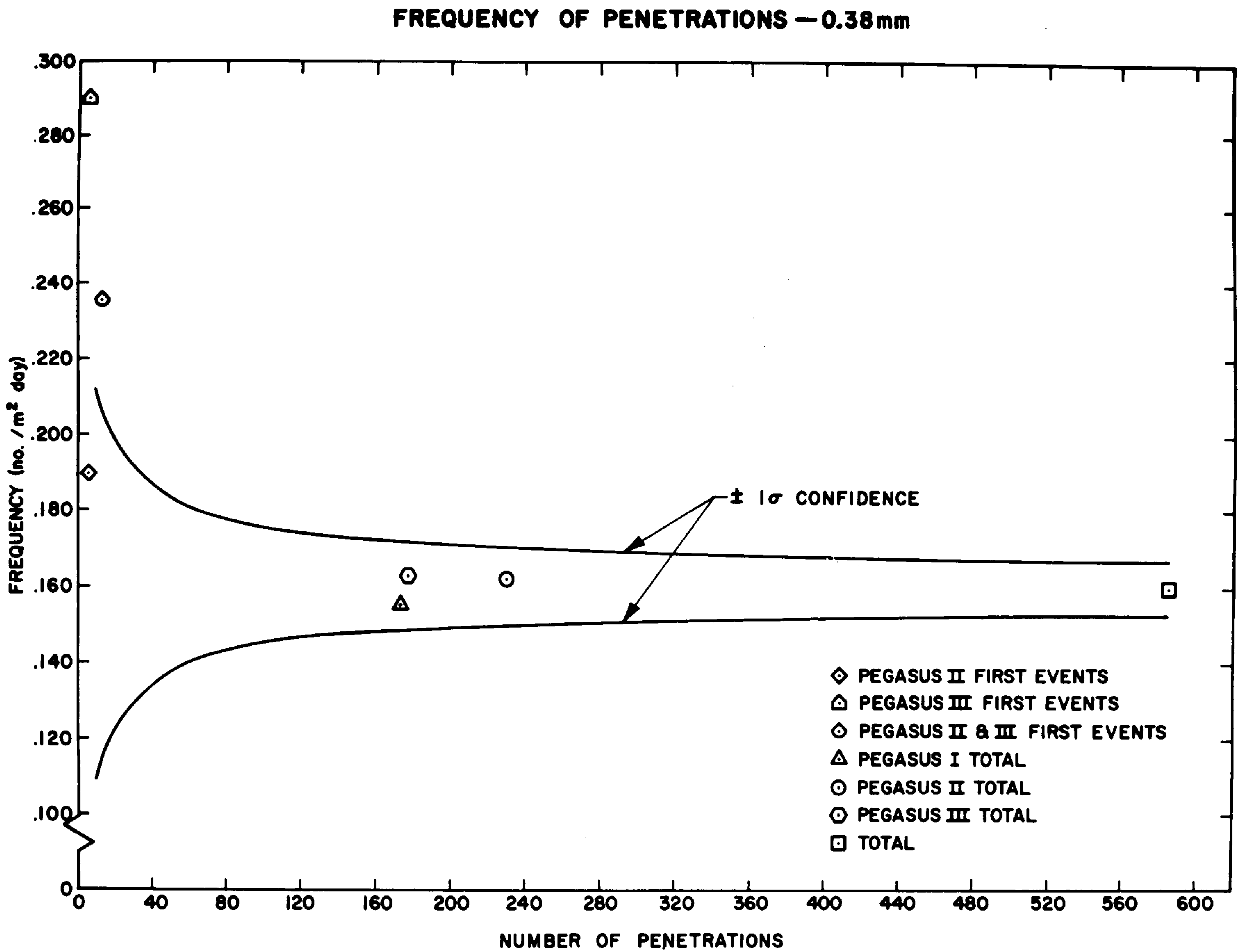

FIGURE 5. COMPARISON OF THE FREQUENCY OF 0.38-MM PANEL PENETRATIONS BETWEEN INITIAL AND TOTAL EVENTS

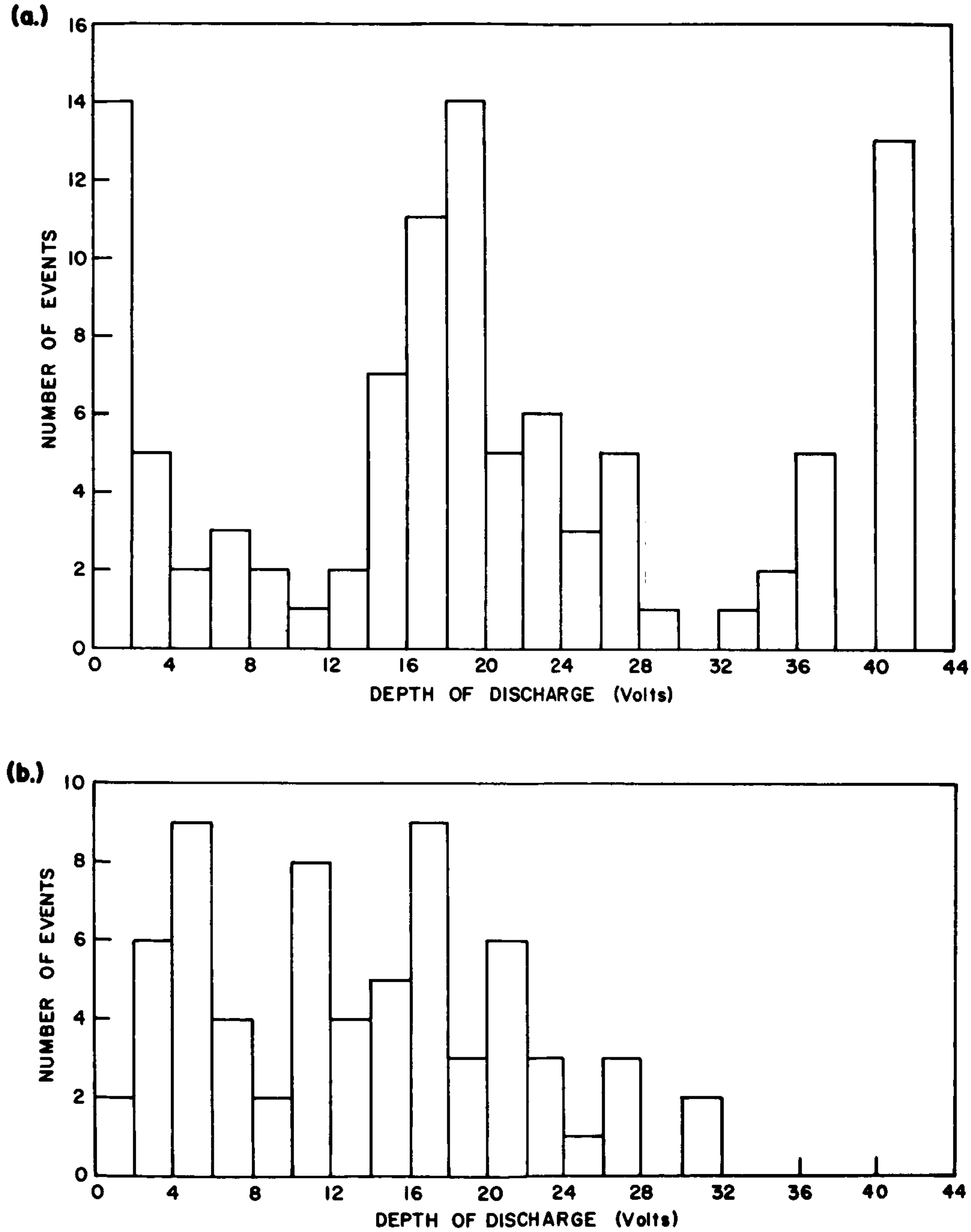

FIGURE 6. DISTRIBUTION OF DEPTHS OF DISCHARGE OBSERVED FROM LABORATORY TESTS ON THE (a) 0.4-MM PANELS AND (b) 0.038-MM PANELS

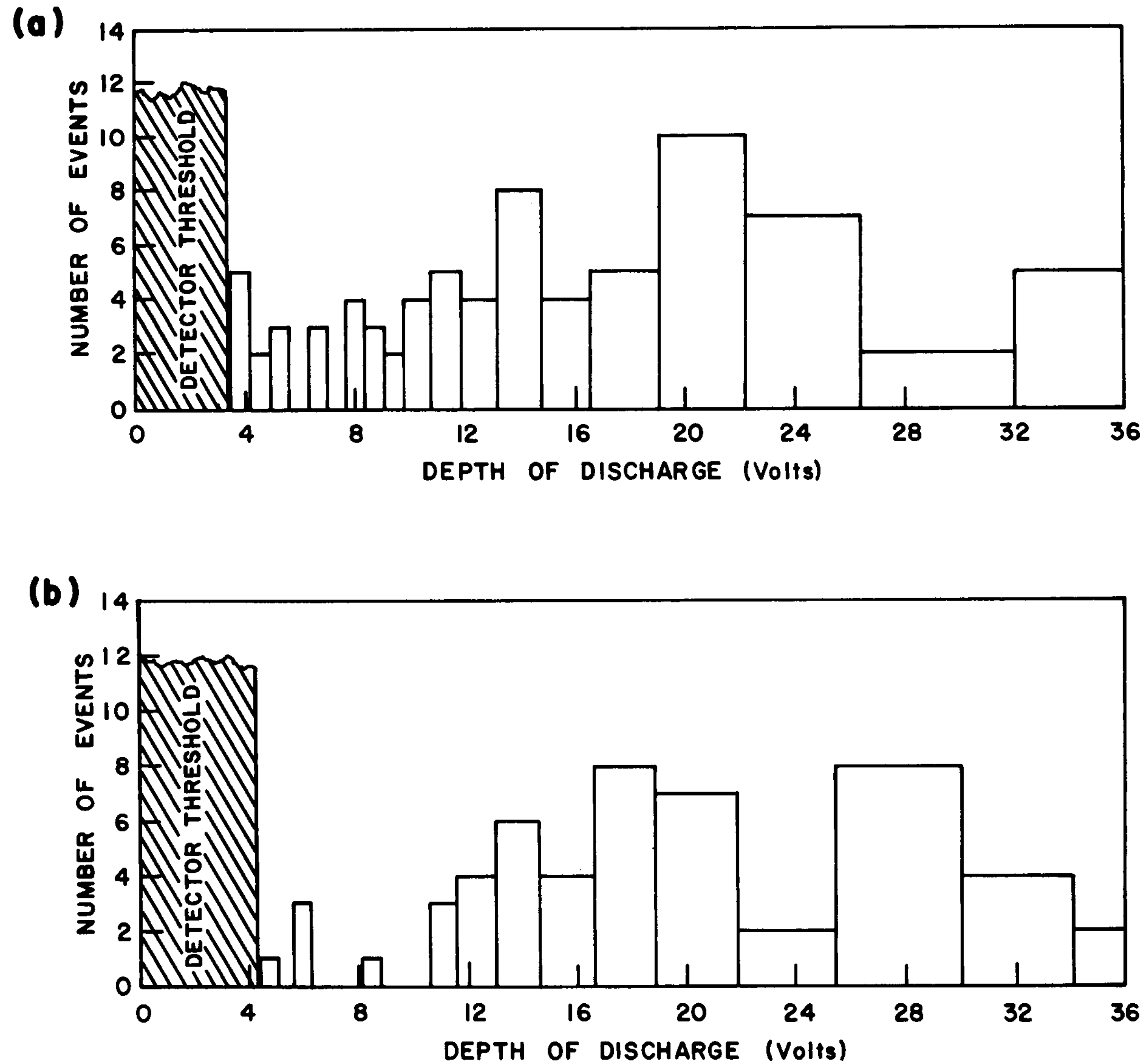

FIGURE 7. DISTRIBUTION OF THE DEPTHS OF DISCHARGE OBSERVED ON THE (a) PEGASUS II 0.4-MM PANELS, (b) PEGASUS III 0.4-MM PANELS

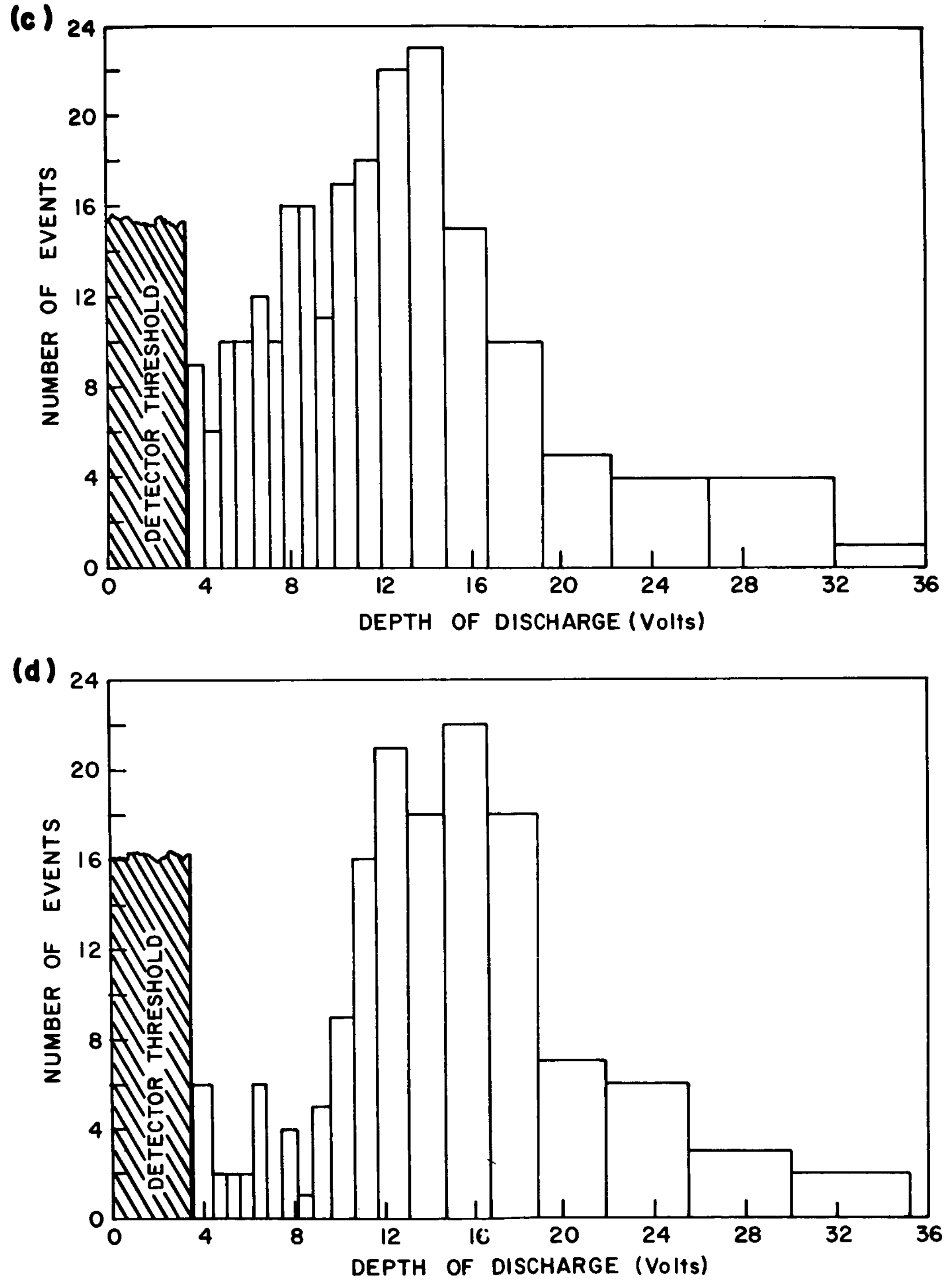

FIGURE 7. (c) PEGASUS II 0.038-MM PANELS, AND (d) PEGASUS III 0.038-MM PANELS. The results from the 0.2-mm panels are not shown as the observed penetrations number too few to result in a meaningful distribution.

Figures 7a, 7b, 7c, and 7d portray the actual results observed by the Pegasus satellites. The satellites record the recharge time after a penetration, and this value must be converted to the corresponding value of depth of discharge. This is accomplished using the recharge time observed when various panels were discharged to selected depths in pre-flight tests. The relation between discharge depth and recharge time is not linear, which somewhat distorts the abscissa. Also, there is some spread in the observed recharge times resulting from a given discharge. Therefore, the precision with which depth of discharge can be inferred from recharge time is not high, but is sufficient to determine whether the distribution of discharge voltages resulting from actual meteoroids is similar to or vastly different from laboratory tests.

Since there does not appear to be significant differences between the observed distributions and the laboratory distributions, the acceptance rates established in the laboratory will be considered applicable. These rates are 86, 86, and 82 percent for the 0.038-mm, 0.2-mm and 0.4-mm panels, respectively. Applying these factors to the observed rates, the fluxes are $.00487/m^2$ day for the 0.4-mm detectors, $.0209/m^2$ day for the 0.2-mm detectors, and $0.188/m^2$ day for the 0.038mm detectors.

ANALYSIS OF THE DATA

The correlation of Pegasus data with temporal effects or with known meteoric activity is of considerable interest. The temporal effects include possible diurnal and seasonal effects upon the data.

In order to isolate a possible diurnal effect, the universal time of each penetration has been converted into local (or solar) time. This system may be visualized with 0 hours representing the antisolar direction; 6 hours, the apex of the earth's motion about the sun; 12 hours, the solar direction; and 18 hours, the antapex of the earth's motion. Hence, the position of the satellite with respect to the earth and sun may be found at any moment of meteoroid impingement. In order to discern whether activity was prevalent in any preferred satellite location, the solar day was divided into local time zones of three hours each.

The results of this analysis are presented in Figures 8a, 8b, 9a, 9b, and 9c. Figures 8a and 8b combine from Pegasus II and Pegasus III, respectively the 0.038-mm and 0.4-mm panel data. It is apparent from these figures that Pegasus II observes a slight abundance of penetrations in the region 9 to 12 hours, and a low number of penetrations in the region of 21 to 24 hours; Pegasus III records no such effect, and its results are distributed uniformly.

When the combined data from Pegasus II and III are separated according to panel thickness, as in Figures 9a and 9b, the 0.038mm data portray an abundance of penetrations in the 15 to 18-hour region and a low number of penetrations in the

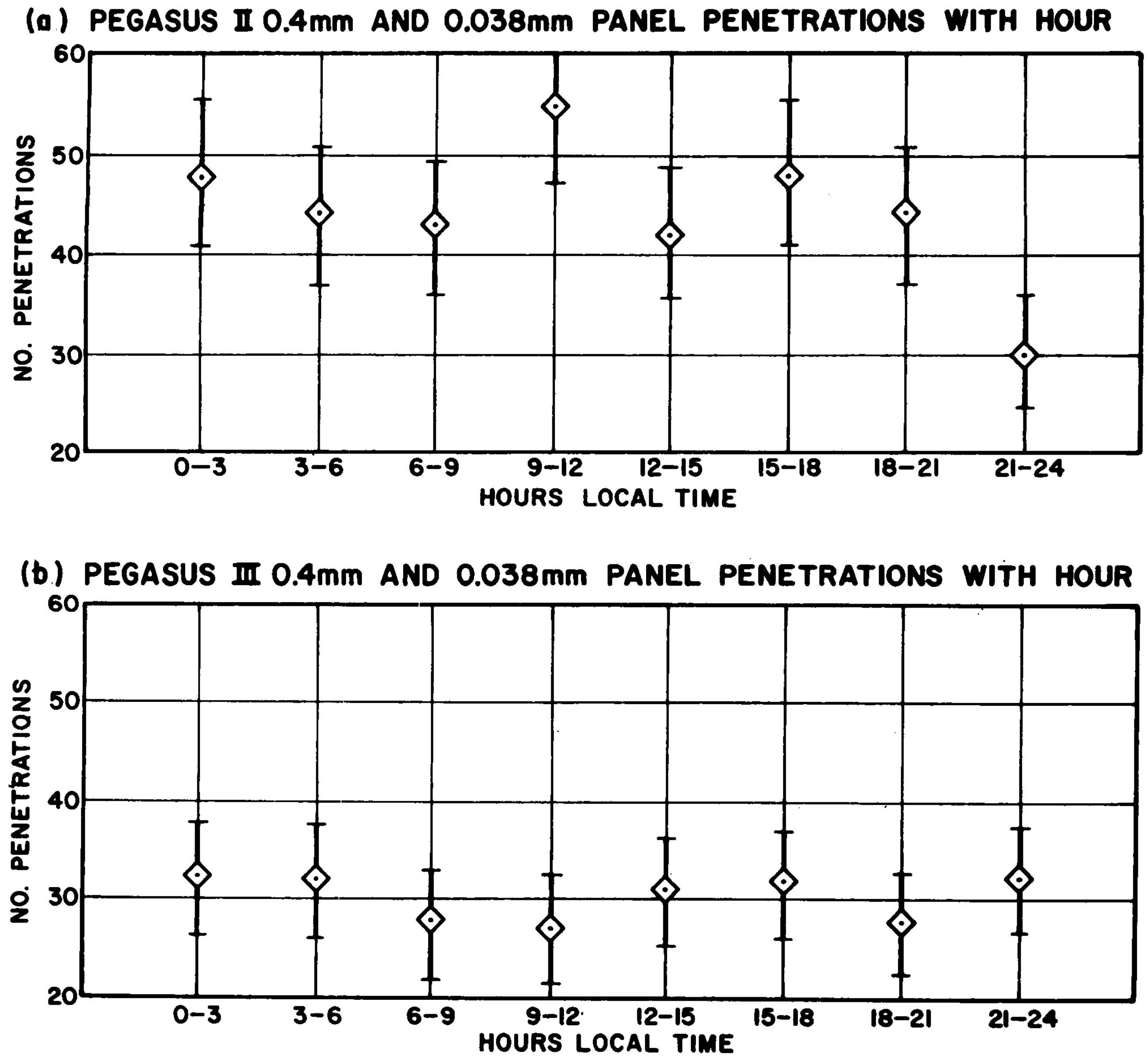

FIGURE 8. DISTRIBUTIONS OF PANEL PENETRATIONS WITH HOURS OF LOCAL TIME

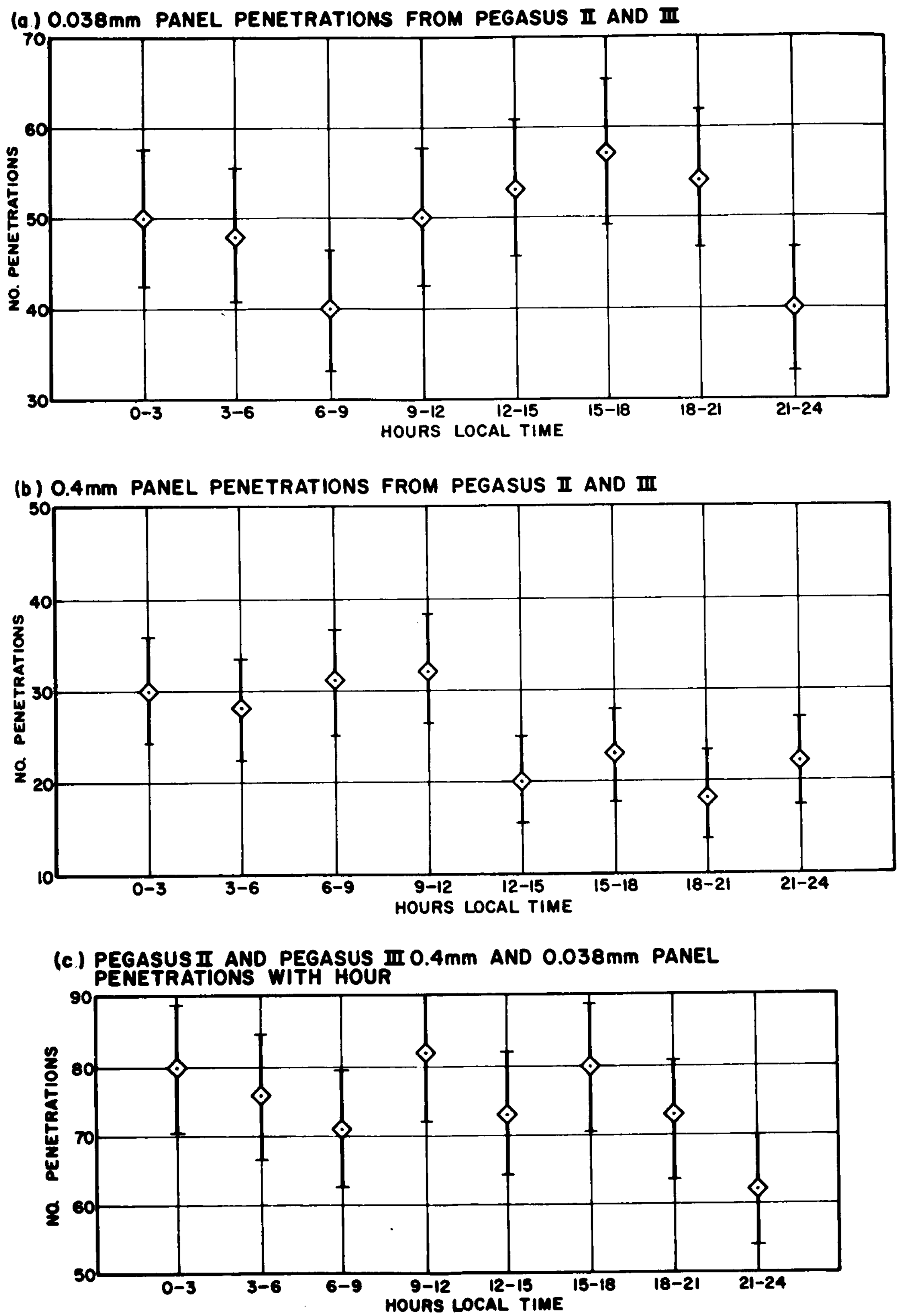

FIGURE 9. DISTRIBUTIONS OF PANEL PENETRATIONS WITH HOURS OF LOCAL TIME

6 to 9-hour and 21 to 24-hour regions. The 0.4-mm data show consistently higher results from 0 to 12 hours and consistently lower results from 12 to 24 hours. Due to the longer lifetime of Pegasus II, its data dominate the results shown in these figures. Furthermore, the variations observed may be statistical. Finally, in Figure 9c, the data from both satellites and both panel thicknesses are combined. The lack of correlation between the fluctuations observed in the data of the two satellites tends to smooth the distribution of penetrations.

In order to isolate a seasonal trend upon the data, a monthly flux was computed for each satellite, and the results summarized in Figures 10a, 10b, and 10c. Figure 10a displays the monthly flux of the 0.038-mm panel data from Pegasus II and III, while Figure 10b portrays the monthly flux of the 0.4-mm panel data from the two satellites. Finally, in Figure 10c, the valid 0.038-mm panel data from Pegasus I are added to the results of Pegasus II and III. The general decrease in flux indicated in Figure 10a is moderated by the addition of the Pegasus I data. Furthermore, it is not apparent from the 0.4-mm panel data from Pegasus I and Pegasus II that any statistically meaningful trend exists with these results. Therefore, it may be concluded that no seasonal effect has been observed with any certainty during the months from June to December.

In order to determine if a possible correlation exists between the results of Pegasus and major, permanent meteor showers, the results from Pegasus II and III were examined to find intervals over which the flux of penetrations deviated from the overall flux by at least 2σ. The lack of 0.4-mm data, the orientation, and the anomalous behavior of Pegasus I precludes its use in this analysis. The results of the analysis are recorded in Figure 11.

The distribution with time of the 0.038-mm data from both satellites is recorded in Figure 11a. Figures 11b and 11c portray those periods exhibiting high flux values for Pegasus II and Pegasus III, respectively. Horizontal bars denote the period in which the number of actual penetrations exceeds the expected number by at least $2\ \sigma$. It may be seen that each satellite recorded two periods of excessive activity. Pegasus II recorded high penetration rates throughout the periods of June 6 through 12 and October 2 through 4. The first of these periods coincides with two meteor showers, the ξ Perseids and the Arietids, as may be seen when Figures 11b and 11g are compared. The second period, however, coincides with no major known shower. Pegasus III recorded excessive activity during the periods August 21 through 29 and October 18 through 23; the former period does not coincide with any major shower; the latter period occurs simultaneously with the Orionids.

It should be noted that when the 0.038-mm panel data from the two satellites are combined as in Figure 11d, the penetration rate does not exceed the average rate by $2\ \sigma$ for any period. There is no period during which the combined data from both satellites indicate excessive activity. Furthermore, the orientation

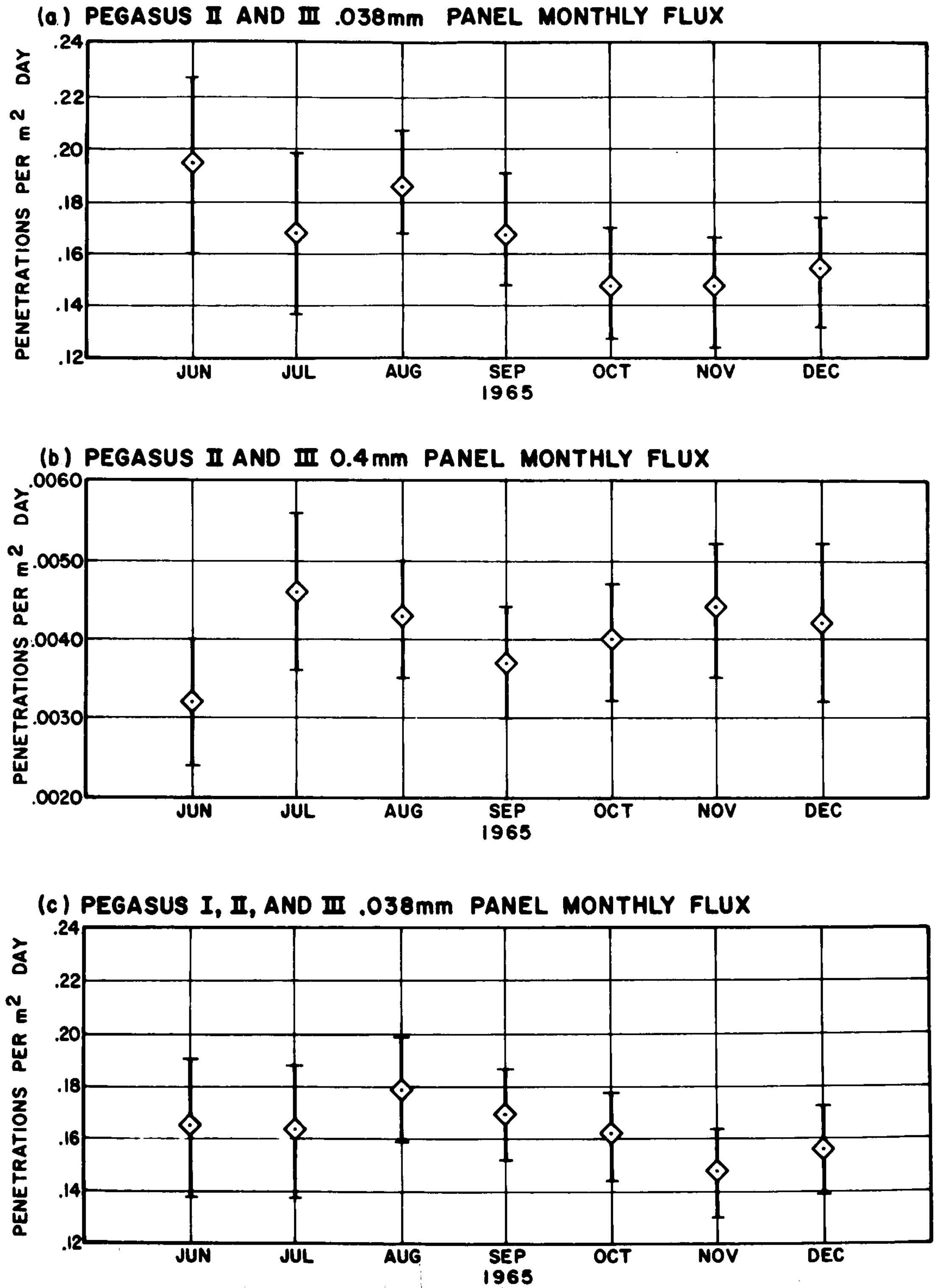

FIGURE 10. MONTHLY DISTRIBUTIONS OF METEOROID FLUX

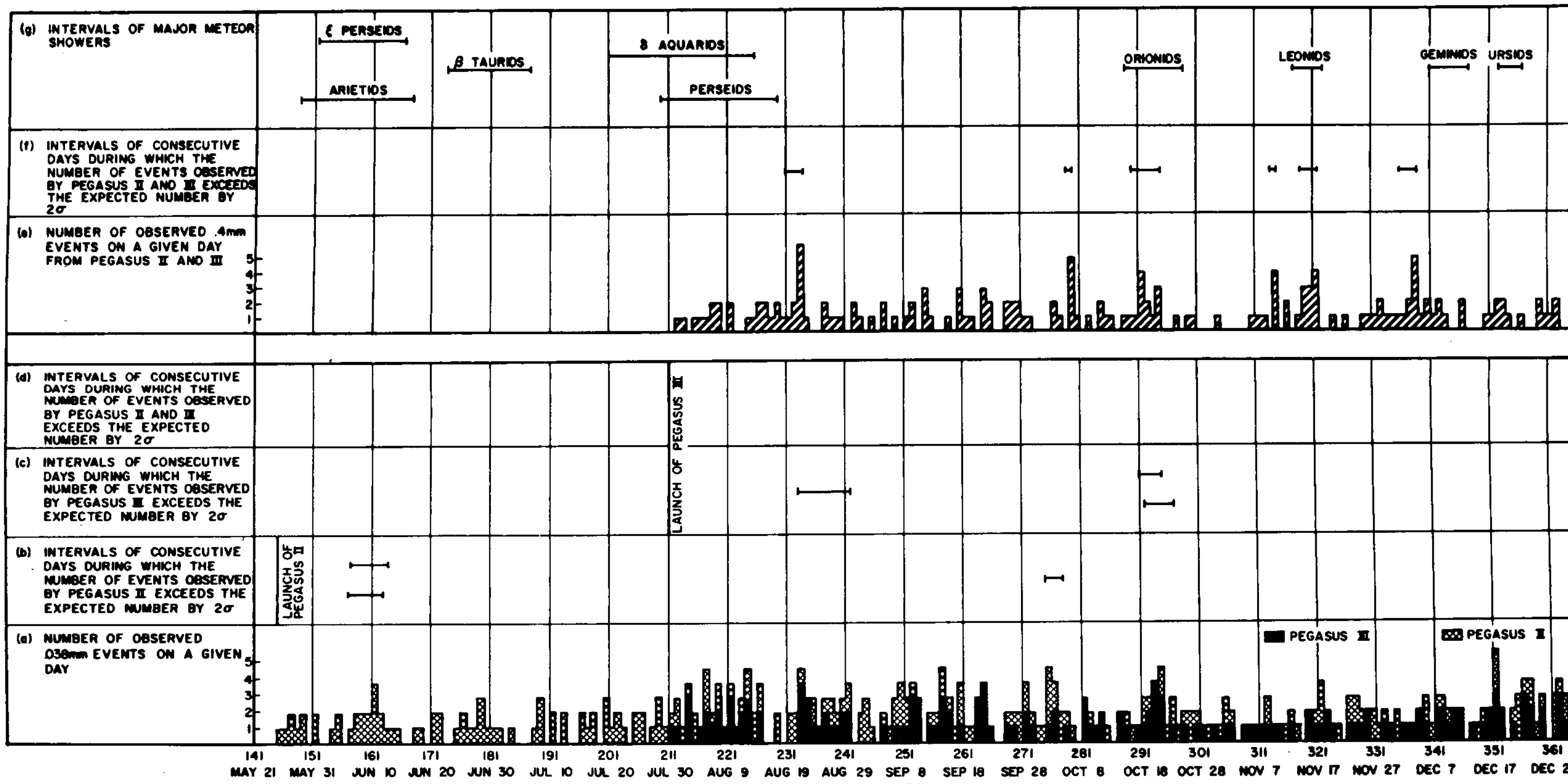

FIGURE 11. DAILY DISTRIBUTION OF METEOROID PENETRATIONS IN COMPARISON WITH PERIODS OF MAJOR PERMANENT METEOR SHOWERS

of the two satellites is sufficiently random to expect both to observe any shower activity. It should be mentioned, however, that the period June 6 through 12 throughout which Pegasus II displayed high activity preceded the launch of Pegasus III and is therefore omitted from this analysis.

In Figure 11e the distribution with time of the combined 0.4-mm panel data from Pegasus II and III is considered. The data are not separated by satellite due to the relatively small number of penetrations observed by the 0.4-mm panels. Furthermore, only the period after the launch of Pegasus III is considered in the figure. Figure 11f portrays the periods during which the combined 0.4-mm panels recorded high activity exceeding the 2 σ criteria stated above. Horizontal bars, as before, denote the periods of excessive activity. These panels recorded six periods of high activity occurring August 19 through 21, October 6, October 17 through 21, November 10, November 15 through 17, and December 1 through 3. Two of these periods occur simultaneously with major meteor showers. The high flux during October 18 through 22 coincides with the Orionid shower and is reflected in the Pegasus III 0.038-mm panel data. The number of penetrations during November 15 through 17 shows a marked increase exceeding the expected number for that period by 3 σ. This period of high activity is coincident with the Leonid shower. A third period of high activity occurring August 19 through 21 does not coincide with a major shower, but is reflected in the 0.038-mm panel data from Pegasus III.

From this analysis it is evident that periods of high activity (exceeding expected activity by 2 σ) do exist. Some, but certainly not all, of these periods coincide with major meteor showers. Furthermore, variations exceeding the 2 σ and 3 σ limits are expected on purely statistical grounds. Therefore, it cannot be said with any certainty that the Pegasus meteoroid detectors observed any major meteor showers, although the high flux of penetrations during the periods coincident with the Leonid and Orionid showers raises the possibility.

COMPARISON OF PEGASUS DATA WITH MODELS OF FLUX AND PENETRATION

Figure 12 shows how the Pegasus data stands in relation to various estimates of the meteoroid hazard. Although the 0.2-mm and 0.4-mm points fall fairly close to Whipple's "Best Estimate"[2], it is apparent that the slope implied by these two points in this region is quite different from that predicted. Since Whipple's predictions are extrapolated from astronomical observations of much larger meteoroids, it is not surprising that such a difference should exist.

The effective thickness of the 0.038-mm panels is taken as 0.050 mm. This value was obtained by adding the 0.012-mm mylar dielectric thickness that must also be penetrated to the 0.038-mm thickness of aluminum. This amount should also be added to the 0.2- and 0.4-mm thickness, but such a correction is small and is less than the thickness tolerance of the aluminum sheet.

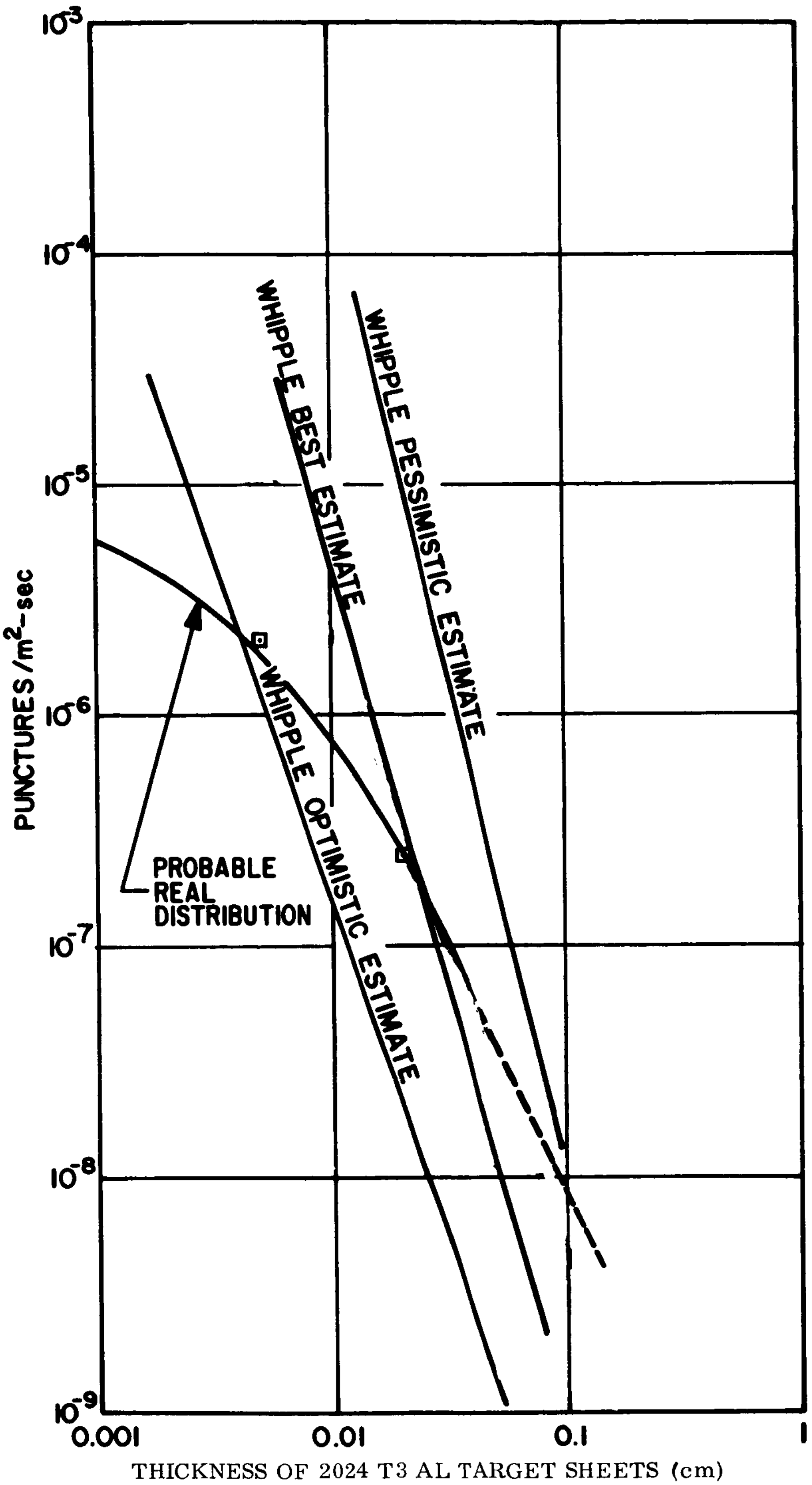

FIGURE 12. THE PEGASUS DATA POINTS IN RELATION TO OTHER MODELS OF FLUX AND PENETRATION

It may be noted that the slope of the cumulative mass-flux obtained from Explorer 16 and 23, Pegasus, radar and photographic measurements has been observed to steepen monotonically with increasing mass. An analysis of this varying slope has been completed and will be published separately .* The results of this study are indicated by the curve labeled "Probable Real Distribution."

CONCLUSIONS

A criterion has been set forth eliminating subjective judgment concerning the validity of penetration data. On this basis the meteoroid penetration fluxes for the different target sheet thicknesses from the three satellites were computed. The results were then corrected for possible lost penetrations to give fluxes of $.00487/m^2$ day for the 0.4-mm detectors, $.0209/m^3$ day for the 0.2-mm detectors, and $0.188/m^2$ day for the 0.038-mm detectors.

The satellite results were examined for possible temporal effects or effects from major meteor showers. It was concluded that although the possibility of such trends exist, there was no conclusive evidence of any significant trend whether diurnal, seasonal, or due to meteoric activity.

The data were then compared to other models of flux and penetration. The 0.2-mm and 0.4-mm points lie between the Whipple Best Estimate and Pessimistic Estimate. However, the slope implied by the Pegasus points is not as steep as predicted by the Whipple model, and if the Pegasus data is extrapolated to thicker materials, the resulting puncture rate is higher than predicted by any model. Since there is evidence that the slope steepens with increasing mass, a straight line extratrapolation is probably too pessimistic, but can be taken as an upper limit. A detailed discussion of the best present estimate of the meteoroid environment obtained from satellite, radar, and photographic data is published separately.

* Naumann, R. J.: The Near Earth Meteoroid Environment. NASA TN (to be published).

REFERENCES

1. Naumann, R. J.: Pegasus Satellite Measurements of Meteoroid Penetration (Feb 16 - July 20, 1965). NASA TM X-1192, Marshall Space Flight Center, Huntsville, Alabama, December 1965.

2. Whipple, Fred L.: On Meteoroids and Penetration. J. Geophys. Res. Vol. 68, No. 17, Sept. 1963, pp. 4929-39.

APPENDIX

Table AI
PEGASUS I PANEL-HIT DISTRIBUTION

Wing	Panel	Z	Thickness of Panel (mm)	Number of Hits	Active Initial Area (meters^2)	Active Area Dec 31 (meters^2)
-	007	-	0.038	39	.930	.930
+	007	-	0.038	15	.920	.920
-	103	+	0.038	26	.930	.930
+	103	+	0.038	24	.914	.914
-	105	+	0.038	18	.920	.920
+	105	+	0.038	2	.930	0
-	106	-	0.038	0	0	0
+	106	-	0.038	29	.930	.930

Table AII
PEGASUS II PANEL-HIT DISTRIBUTION *

Wing	Panel	Z	Thickness of Panel (mm)	Number of Hits	Active Initial Area (meters^2)	Active Area Dec 31 (meters^2)
+	103	+	0.038	37	.931	.931
+	105	+	0.038	37	.931	.931
+	106	-	0.038	37	.931	.931
+	007	-	0.038	0	0	0
+	111	+	0.2	7	2.779	2.316
+	112	-	0.2	3	2.808	2.340
+	013	+	0.2	2	1.404	0
+	114	+	0.4	1	3.715	0
+	015	-	0.4	1	3.744	0
+	016	+	0.4	1	3.715	3.715
+	121	-	0.4	2	3.744	3.276
+	122	+	0.4	3	2.808	2.340
+	023	-	0.4	1	2.779	2.779
+	124	+	0.4	9	3.744	3.276
+	025	-	0.4	2	3.715	0
+	026	+	0.4	2	3.715	3.715
+	130	-	0.4	3	3.744	3.744
+	031	+	0.4	3	3.715	3.251

Table AII (Continued)
PEGASUS II PANEL-HIT DISTRIBUTION

Wing	Panel	Z	Thickness of panel (mm)	Number of Hits	Active Initial Area (meters^2)	Active Area Dec 31 (meters^2)
+	032	-	0.4	1	3.744	0
+	034	+	0.4	4	3.744	3.276
+	141	-	0.4	3	3.715	0
+	142	+	0.4	1	3.744	3.276
+	043	-	0.4	1	3.715	0
+	144	+	0.4	2	3.715	0
+	045	-	0.4	1	3.744	3.744
+	046	+	0.4	2	3.744	3.744
+	150	-	0.4	4	3.715	3.715
+	051	+	0.4	2	2.400	1.920
+	052	-	0.4	0	0	0
+	054	+	0.4	3	3.566	3.120
+	160	-	0.4	1	3.620	0
+	061	-	0.2	0	0	0
-	103	+	0.038	35	.931	.931
-	105	+	0.038	25	.931	.931
-	106	-	0.038	30	.931	.931
-	007	-	0.038	27	.931	.931
-	111	+	0.2	7	3.744	1.853
-	112	-	0.2	7	3.715	0
-	114	+	0.4	4	3.744	1.853
-	015	-	0.4	4	3.715	3.251
-	016	+	0.4	1	3.744	3.744
-	121	-	0.4	5	3.715	3.715
-	122	+	0.4	3	2.779	2.316
-	023	-	0.4	5	3.744	3.276
-	124	+	0.4	2	3.715	0
-	025	-	0.4	1	2.808	2.340
-	026	+	0.4	1	3.744	3.744
-	130	-	0.4	1	3.715	3.715
-	031	+	0.4	3	3.744	3.744
-	032	-	0.4	3	3.715	3.251
-	034	+	0.4	3	3.715	3.715
-	141	-	0.4	3	3.744	2.868
-	142	+	0.4	4	3.715	3.715
-	043	-	0.4	3	3.744	3.744
-	144	+	0.4	0	3.744	3.744

Table AII (Concluded)
PEGASUS II PANEL-HIT DISTRIBUTION

Wing	Panel	Z	Thickness of Panel (mm)	Number of Hits	Active Initial Area (meters^2)	Active Area Dec 31 (meters^2)
-	045	-	0.4	2	3.744	3.251
-	046	+	0.4	3	3.715	3.251
-	051	+	0.4	5	2.779	1.853
-	052	-	0.4	4	2.808	2.808
-	054	+	0.4	2	3.620	0
-	150	-	0.4	3	3.715	3.251
-	160	-	0.4	3	3.566	3.566

* See Figure 13

Table AIII
PEGASUS III PANEL-HIT DISTRIBUTION *

Wing	Panel	Z	Thickness of Panel (mm)	Number of Hits	Active Initial Area (meters^2)	Active Area Dec 31 (meters^2)
+	103	+	0.038	23	.931	.931
+	105	+	0.038	19	.931	.931
+	106	-	0.038	22	.931	.931
+	007	-	0.038	0	0	0
+	111	+	0.2	3	2.789	0
+	112	-	0.2	5	2.808	0
+	013	+	0.2	1	1.404	0
+	114	+	0.4	2	3.715	0
+	015	-	0.4	1	3.744	3.744
+	016	+	0.4	1	3.175	0
+	121	-	0.4	0	3.744	0
+	122	+	0.4	1	2.808	2.808
+	023	-	0.4	2	2.779	2.779
+	124	+	0.4	3	3.744	3.744
+	025	-	0.4	3	3.715	3.251
+	026	+	0.4	1	3.715	0
+	130	-	0.4	1	3.744	0
+	031	+	0.4	1	3.715	3.251
+	032	-	0.4	4	3.744	3.744
+	034	+	0.4	2	3.744	3.744
+	141	-	0.4	3	3.715	3.715

Table AIII (Continued)
PEGASUS III PANEL-HIT DISTRIBUTION

Wing	Panel	Z	Thickness of Panel (mm)	Number of Hits	Active Initial Area (meters^2)	Active Area Dec 31 (meters^2)
+	142	+	0.4	2	3.744	0
+	043	-	0.4	0	3.715	3.715
+	144	+	0.4	1	3.715	3.715
+	045	-	0.4	1	3.744	3.744
+	046	+	0.4	1	3.744	0
+	150	-	0.4	2	3.715	3.251
+	051	+	0.4	0	.468	.468
+	052	-	0.4	0	0	0
+	054	+	0.4	0	3.566	3.566
+	160	-	0.4	1	3.620	0
+	061	-	0.2	0	0	0
-	103	+	0.038	28	.931	.931
+	105	+	0.038	17	.931	.931
+	106	-	0.038	22	.931	.931
-	007	-	0.038	28	.931	.931
-	111	+	0.2	5	3.744	0
-	112	-	0.2	1	3.715	0
-	114	+	0.4	1	3.744	3.744
-	015	-	0.4	2	3.715	0
-	016	+	0.4	0	3.744	3.744
-	121	-	0.4	1	3.715	0
-	122	+	0.4	0	2.779	2.779
-	023	-	0.4	1	3.774	0
-	124	+	0.4	4	3.715	3.251
-	025	-	0.4	1	2.808	2.808
-	026	+	0.4	0	3.744	0
-	130	-	0.4	2	3.715	3.251
-	031	+	0.4	4	3.744	0
-	032	-	0.4	0	3.715	3.715
-	034	+	0.4	8	3.715	3.787
-	141	-	0.4	2	3.744	3.744
-	142	+	0.4	2	3.715	3.251
-	043	-	0.4	0	3.744	3.744
-	144	+	0.4	1	3.744	0
-	045	-	0.4	5	3.744	1.873
-	046	+	0.4	3	3.715	3.251
-	051	+	0.4	0	.922	.922

Table AIII (Concluded)
PEGASUS III PANEL-HIT DISTRIBUTION

Wing	Panel	Z	Thickness of Panel (mm)	Number of Hits	Active Initial Area (meters^2)	Active Area Dec 31 (meters^2)
-	052	-	0.4	1	.936	.936
-	054	+	0.4	3	3.620	0
-	150	-	0.4	2	3.715	3.715
-	160	-	0.4	2	3.566	3.566

* See Figure 13

PEGASUS DETECTOR PANELS

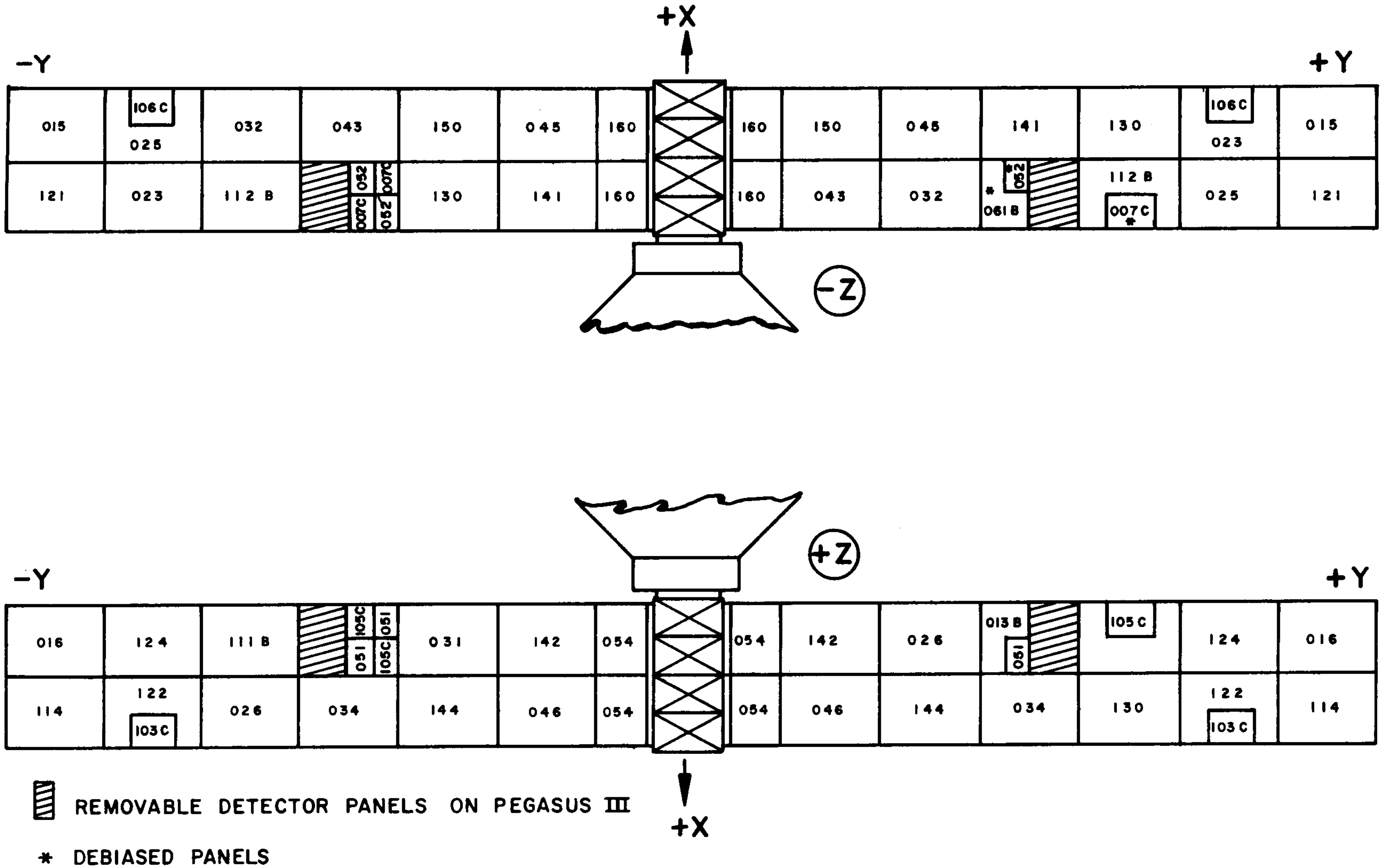

FIGURE 13. SCHEMATIC OF PEGASUS WINGS SHOWING LOCATIONS OF VARIOUS LOGIC GROUPS. The letter C after the logic group identification indicates 0.038-mm panels; B denotes 0.2-mm panels, no letter indicates 0.4-mm panels.

"The aeronautical and space activities of the United States shall be conducted so as to contribute . . . to the expansion of human knowledge of phenomena in the atmosphere and space. The Administration shall provide for the widest practicable and appropriate dissemination of information concerning its activities and the results thereof."

—NATIONAL AERONAUTICS AND SPACE ACT OF 1958

NASA SCIENTIFIC AND TECHNICAL PUBLICATIONS

TECHNICAL REPORTS: Scientific and technical information considered important, complete, and a lasting contribution to existing knowledge.

TECHNICAL NOTES: Information less broad in scope but nevertheless of importance as a contribution to existing knowledge.

TECHNICAL MEMORANDUMS: Information receiving limited distribution because of preliminary data, security classification, or other reasons.

CONTRACTOR REPORTS: Technical information generated in connection with a NASA contract or grant and released under NASA auspices.

TECHNICAL TRANSLATIONS: Information published in a foreign language considered to merit NASA distribution in English.

TECHNICAL REPRINTS: Information derived from NASA activities and initially published in the form of journal articles.

SPECIAL PUBLICATIONS: Information derived from or of value to NASA activities but not necessarily reporting the results of individual NASA-programmed scientific efforts. Publications include conference proceedings, monographs, data compilations, handbooks, sourcebooks, and special bibliographies.

Details on the availability of these publications may be obtained from:

SCIENTIFIC AND TECHNICAL INFORMATION DIVISION

NATIONAL AERONAUTICS AND SPACE ADMINISTRATION

Washington, D.C. 20546